Phase retrieval in x-ray lensless holography by reference beam tuning

Diling Zhu,[1,2,*] Benny Wu,[1,2] Ramon Rick,[1,2] Joachim Stöhr,[2,3] and Andreas Scherz[2]

[1]*Department of Applied Physics, Stanford University, Via Pueblo Mall, Stanford, California 94305, USA*
[2]*Stanford Institute for Material & Energy Science, SLAC National Accelerator Laboratory, 2575 Sand Hill Road, Menlo Park, California 94025, USA*
[3]*Linac Coherent Light Source, SLAC National Accelerator Laboratory, 2575 Sand Hill Road, Menlo Park, California 94025, USA*
[*]*Corresponding author: dlzhu@stanford.edu*

Received April 28, 2009; revised July 21, 2009; accepted July 29, 2009;
posted August 4, 2009 (Doc. ID 110542); published August 21, 2009

We show the ability to determine the relative phase between the object and a reference scatterer by tuning the overall intensity and phase of the reference wave. The proposed reference-guided phase retrieval algorithm uses the relative phase as a constraint to iteratively reconstruct the object and the reference simultaneously, and thus does not require precisely defined reference structures. The algorithm also features rapid and reliable convergence and overcomes the uniqueness problem. The method is demonstrated by a soft-x-ray coherent imaging experiment that utilizes a large micrometer-sized reference structure that can be turned on and off, yielding an object image with resolution close to the reconstruction pixel size of 21 nm.

OCIS codes: 110.7440, 090.0090, 340.7460, 100.5070.

At the heart of holography lies the relative phase, which is encoded in the interference fringes produced by coherent superposition of the reference and the object waves. The object phase can be recovered to the extent of the knowledge of the reference phase, but in the x-ray regime this has been impeded by the lack of suitable optics to create and control reference beams. Consequently, most efforts in x-ray holography have pursued lensless approaches. In the past decade, a few studies have demonstrated the power of utilizing nanoscale reference structures [1–3]. However, in these approaches the image resolution and the quality of the image reconstruction depend on the ability to create well-defined, ultrasmall reference structures, typically produced by nanofabrication.

In this Letter we introduce an alternative by incorporating traditional phase retrieval [4,5] into x-ray holography. Instead of relying on the precise fabrication and knowledge of the reference structure, we use an extended reference whose transmissivity can be tuned, e.g., by changing the incident wavelength. Recording multiple holograms with varying overall reference intensity and phase allows us to determine the relative holographic phase. This phase information serves as a Fourier domain constraint in an iterative algorithm to recover the image. The proposed reference-guided phase retrieval (RPR) method deconvolves the object and the reference simultaneously. The holographic constraints ensure that the convergence is rapid and independent of the signal-to-noise ratio (SNR). This is in contrast to previous work [3,6–8], where improvements in the resolution beyond the reference size are achievable by subsequent application of phase retrieval algorithms only when the SNR is sufficient. Our technique builds on earlier work that demonstrated multiple-wavelength anomalous diffraction near absorption edges for the reconstruction of nonperiodic objects [9]. Here, we generalize this concept and show that it is suitable for recovering phases in a broad range of lensless imaging scenarios.

Consider the exit wave at the sample plane taking the form $\psi(x,y)=\psi_o(x,y)+\xi\psi_r(x,y)$, where ψ_o and ψ_r describe the scattered waves from the object and the reference, respectively, and the complex-valued parameter $\xi=|\xi|e^{i\theta_\xi}$ represents a tunable reference. In the Fraunhofer diffraction regime the wave field can be written as

$$\Psi(p,q)=\Psi_o(p,q)+\xi\Psi_r(p,q), \tag{1}$$

where $\Psi(p,q)$ denotes the Fourier transform of $\psi(x,y)$, and (p,q) are the reciprocal space coordinates. The diffraction intensity is given by

$$I_\xi(p,q)=|\Psi_o|^2+|\xi|^2|\Psi_r|^2+2|\Psi_o||\Psi_r||\xi|\cos(\Delta\Phi+\theta_\xi), \tag{2}$$

where $\Delta\Phi(p,q)=\Phi_o(p,q)-\Phi_r(p,q)$ is the relative phase of the object and the reference wave in reciprocal space. By tuning $\xi=\xi_1,\xi_2,\xi_3,\ldots$ and recording three or more diffraction patterns as a first step, the three unknowns $|\Psi_o|$, $|\Psi_r|$, and $\Delta\Phi$ can be determined for each point (p,q). These components form the Fourier domain constraints for the RPR routine, as shown in Fig. 1.

As a second step, the RPR routine iteratively deconvolves the object and the reference by determining their individual phases Φ_o and Φ_r. As shown in Fig. 1, the algorithm starts with a random guess for Φ_o and uses the error reduction method [4] on the object to update the object's phase to $\Phi_o'(i)$. Because of the Fourier domain constraints, the phase of the reference is updated as well, i.e., $\Phi_r'(i)=\Phi_o'(i)-\Delta\Phi$. Applying another error reduction cycle, this time on the reference, gives $\Phi_r(i+1)$ and $\Phi_o(i+1)=\Delta\Phi+\Phi_r(i+1)$. The RPR routine iterates until the update falls below

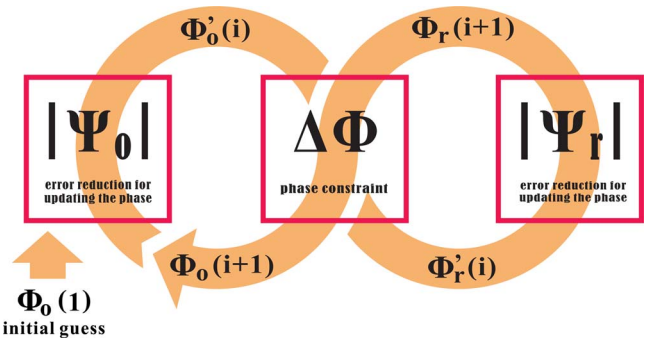

Fig. 1. (Color online) Figure-eight schematic of the reference-guided phase retrieval routine. The algorithm implements the error reduction method alternating between the reference and the object, applying the relative phase $\Delta\Phi$ as an extra Fourier domain constraint.

a given threshold. The embedded error reduction uses the amplitudes $|\Psi_o|$ and $|\Psi_r|$ and support regions defined by the autocorrelations as the Fourier and the object domain constraints.

To investigate the convergence characteristics of the algorithm, we choose a real-valued test structure, shown in Fig. 2(a), with a large circular reference placed next to it. Assuming knowledge of $|\Psi_o|$, $|\Psi_r|$, and $\Delta\Phi$, the convergence is quantified by calculating the normalized mean square error (NMSE) after each iteration i,

$$\mathrm{NMSE}_i = \frac{\Sigma|\psi_i - \psi_o|^2}{\Sigma|\psi_o|^2}, \tag{3}$$

where ψ_o is the convergence limit for the object. The image quality associated with typical NMSE values are shown in Fig. 2(b). The convergence of RPR and the hybrid input-output algorithm (HIO, a standard phase retrieval algorithm for single diffraction patterns [5], using $\beta=0.5$) is shown in Fig. 2(c). The RPR routine reaches a NMSE of 0.1 within 100 Fourier transforms or 25 iterations, following consistent trajectories. On the other hand, HIO requires a tighter support and takes typically around 10^4 iterations to approach the convergence limit, with varying trajectories.

We further introduce shot noise to the simulated holograms for investigating the influence of photon counting noise on RPR. Without loss of generality, we set $\xi=0,1,2$ in Eq. (2) to obtain $|\Psi_o|=\sqrt{I_0}$, $|\Psi_r| = \sqrt{(I_0-2I_1+I_2)/2}$ and the relative phase

$$\Delta\Phi = \arccos\left(\frac{-3I_0+4I_1-I_2}{2\sqrt{2I_0(I_0-2I_1+I_2)}+\sigma}\right), \tag{4}$$

where σ is the Wiener filter parameter to reduce the effect of zero crossings [10]. A correction method is then applied to unwrap the phases [11]. As shown in Fig. 2(d), for total photon counts ranging from 10^6 to 10^{10}, noise lowers the final image quality as reflected in the final NMSE values reached. However, convergence speed is independent of the noise level. In addition, minor deviations in ξ do not affect the outcome of RPR.

As a proof-of-principle experiment, we applied the RPR scheme for nanoscale imaging with Fourier transform holography (FTH) [1,2], using a micrometer-sized reference aperture that can be switched on and off. The object and the reference aperture are placed in the FTH geometry as shown in Fig. 3(a). The test object and a reference are fabricated by focused ion milling. The diameter of the 1 μm circular aperture is chosen for optimum fringe visibility in the hologram. A 200 nm Co film [see Fig. 3(b)] serves as a shutter to switch the reference scattering on ($\xi=1$) and off ($\xi=0$) by changing resonantly the absorption around the Co L_3 edge. After resizing $I_{\xi=1}$ to compensate for the change in wavelength, we derive $|\Phi_o|$, $|\Phi_r|$, and $\Delta\Phi$ from two instead of three holograms: $I_{\xi=0}=|\Psi_o|^2$ and $I_{\xi=1}=|\Psi_o+\Psi_r|^2$, where the autocorrelation and the cross-correlation terms, corresponding to $|\Psi_r|^2$ and $2|\Psi_r||\Psi_o|\cos\Delta\Phi$, are spatially separated in the Fourier transform of $I_{\xi=1}-I_{\xi=0}$.

We performed the experiment at the Stanford Synchrotron Radiation Lightsource (SSRL), beamline 13-3. The two diffraction patterns are recorded at 778 eV($I_{\xi=0}$) and 765 eV($I_{\xi=1}$), as shown in Figs. 3(c) and 3(d) with a 1340×1300 pixel CCD detector placed 250 mm from the sample. Two beam stops of

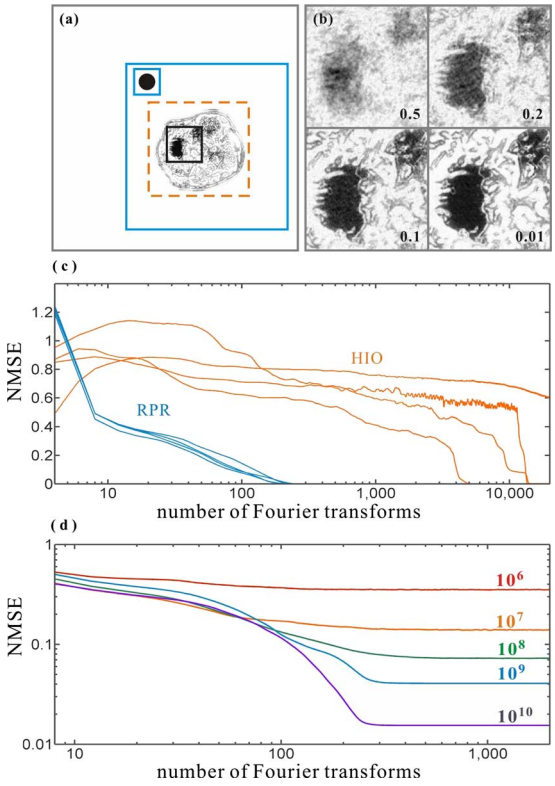

Fig. 2. (Color online) (a) Overview of the test matrix used for the simulations. The blue boxes (solid lines) show the loose RPR support regions for the object and the reference. A tighter support region, orange box (dashed lines), is an important prerequisite for HIO to converge. (b) A magnified region of the sample [black box in (a)] shows the image quality for given NMSE values. (c) Convergence speed of RPR versus HIO runs on noiseless input, four independent runs for each. Note the logarithmic scale on the abscissa. (d) Convergence speed of RPR on data with a total number of detected photons as indicated.

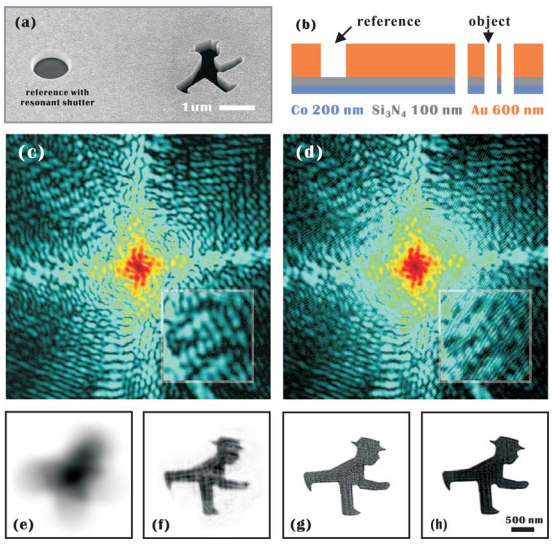

Fig. 3. (Color online) (a) Scanning electron micrograph of the test sample. (b) Illustration of the sample cross section. (c) Diffraction pattern $I_{\xi=0}$ taken at the Co L_3 edge. (d) Diffraction pattern $I_{\xi=1}$ taken before the Co L_3 edge. (e) FTH result and (f) RPR result after 20 iterations. (g) HIO after 100 iterations started with RPR result, and (h) average of 20 independent runs of (g) for eliminating high-frequency noise.

different sizes are used to increase the data dynamic range. The missing low-q part from the smaller beam stop (15 pixels or 250 μm) is smaller than the central node of the holograms and can be iteratively recovered [12], enforcing a support constraint on the obtained autocorrelation.

The RPR reconstruction is shown in Fig. 3(f) for comparison with the reconstruction, Fig. 3(e), obtained with a direct inverse Fourier transform of I_1. While the FTH resolution is limited by the micrometer-sized reference, the object becomes clearly recognizable after 20 iterations of RPR. Fixed support constraints determined by the FTH result are used. The minor artifacts in the RPR reconstruction originate from nodes in Ψ_r where spatial frequencies of the object are not sampled. Within SNR limitations, the missing spatial frequencies can be recovered by HIO initialized with the RPR reconstruction in less than 100 iterations, as shown in Figs. 3(g) and 3(h). Because the object is binary, we determine the resolution from the edge response at the object boundaries. Using the 10%–90% rule, the edge rises within 2 pixels all across the boundary, indicating a resolution of 42 nm or better.

In FTH, smaller reference scatterers are required for achieving higher spatial resolution, but the resulting weaker interference will lead to noisier reconstructions. According to simulations, it takes an exposure time about 500 times longer to achieve the same SNR as we obtained in this experiment, assuming that a 40 nm 100% contrast point scatterer is used. In comparison with previous experiments [2,3], RPR reduces the requirements for both accurate knowledge and precise fabrication of the reference structure. Here, the dimensions of the reference can be selected for optimum fringe visibility in the hologram. Various experimental schemes to obtain multiple holograms for RPR are conceivable. Illumination control can be integrated by other means such as microelectromechanical systems. The tuning of interference can also be achieved by changing object scattering such as in multiple-wavelength anomalous diffraction holography [9], which uses the in-line holography geometry.

In conclusion, we have proposed a phase retrieval algorithm for lensless x-ray microscopy, where the phase difference derived from multiple holograms is introduced as an additional constraint in the Fourier domain. This implementation is reliable and robust against noise and dramatically increases the reconstruction convergence speed. The potential and feasibility of RPR is experimentally verified.

The experiments were carried out at SSRL. Both SSRL and the research program of the authors, funded through the SIMES Center, are supported by the U.S. Department of Energy, Office of Basic Energy Sciences.

References

1. I. McNulty, J. Kirz, C. Jacobsen, E. D. Anderson, M. R. Howells, and D. P. Kern, Science **256**, 1009 (1992).
2. S. Eisebitt, J. Lüning, W. F. Schlotter, M. Lörgen, O. Hellwig, W. Eberhardt, and J. Stöhr, Nature **432**, 885 (2004).
3. S. Marchesini, S. Boutet, A. E. Sakdinawat, M. J. Bogan, S. Bajt, A. Barty, H. N. Chapman, M. Frank, S. P. Hau-Riege, A. Szöke, C. Cui, D. A. Shapiro, M. R. Howells, J. C. H. Spence, J. W. Shaevitz, J. Y. Lee, J. Hajdu, and M. M. Seibert, Nat. Photonics **2**, 560 (2008).
4. R. W. Gerchberg and W. O. Saxton, Optik (Jena) **35**, 237 (1972).
5. J. R. Fienup, Appl. Opt. **21**, 2758 (1982).
6. S. Eisebitt, M. Lögen, and W. Eberhardt, Appl. Phys. Lett. **84**, 3373 (2004).
7. L. Stadler, C. Gutt, T. Autenrieth, O. Leupold, S. Rehbein, Y. Chushkin, and G. Grübel, Phys. Rev. Lett. **100**, 245503 (2008).
8. R. L. Sandberg, D. A. Raymondson, C. La-o-vorakiat, A. Paul, K. S. Raines, J. Miao, M. M. Murnane, H. C. Kapteyn, and W. F. Schlotter, Opt. Lett. **34**, 1618 (2009).
9. A. Scherz, D. Zhu, R. Rick, W. F. Schlotter, S. Roy, J. Lüning, and J. Stöhr, Phys. Rev. Lett. **101**, 076101 (2008).
10. H. He, U. Weierstall, J. C. H. Spence, M. Howells, H. A. Padmore, S. Marchesini, and H. N. Chapman, Appl. Phys. Lett. **85**, 2454 (2004).
11. T. M. Jeong, D.-K. Ko, and J. Lee, Opt. Lett. **32**, 3507 (2007).
12. J. Miao, Y. Nishino, Y. Kohmura, B. Johnson, C. Song, S. H. Risbud, and T. Ishikawa, Phys. Rev. Lett. **95**, 085503 (2005).